frontiers | Frontiers in Energy Research

TYPE Original Research
PUBLISHED 29 October 2024
DOI 10.3389/fenrg.2024.1469739

OPEN ACCESS

EDITED BY
Duo Li,
Newcastle University, United Kingdom

REVIEWED BY
Shenbo Yang,
Beijing University of Technology, China
Xiaolong Yang,
Northeast Electric Power University, China
Hongye Wang,
Dalian University of Technology, China

*CORRESPONDENCE
Jiao Wang,
1677512714@qq.com

RECEIVED 24 July 2024
ACCEPTED 26 September 2024
PUBLISHED 29 October 2024

CITATION
Wang J, Hu J, Bai Z, He H and Tang M (2024) Robust optimization bidding strategy for user-side resource-side participation in the market distribution of electrical energy and peaking ancillary services considering risk expectations and opportunity constraints.
Front. Energy Res. 12:1469739.
doi: 10.3389/fenrg.2024.1469739

Robust optimization bidding strategy for user-side resource-side participation in the market distribution of electrical energy and peaking ancillary services considering risk expectations and opportunity constraints

Jiao Wang[1]*, Jinyan Hu[1], Zhichao Bai[1], Hao He[2] and Mingxin Tang[2]

[1]State Grid Inner Mongolia East Electric Power Company Economic and Technological Research Institute, Hohhot, China, [2]College of Economic and Management, North China Electric PowerUniversity, Beijing, China

Compared to traditional resources, user-side resources are of various types and have more significant uncertainty about their regulatory capacity, leading to difficulties in coordinating decisions about their simultaneous participation in the electric energy and peaking ancillary services markets. This paper proposes a joint bidding decision-making method for the day-ahead electricity energy and peak shaving auxiliary service market based on distributed robust opportunity constraints, which addresses the problem of difficulty in using an accurate probability density distribution to represent the uncertainty process of user-side resources. Firstly, a data-driven method for characterizing the uncertainty of load regulation capacity is investigated, and fuzzy sets are constructed without assuming specific probability distributions of random variables. Then, to minimize the risk expectation of the joint bidding cost on the customer side, a bidding strategy that considers the uncertainty is proposed. Finally, an example simulation verifies the reasonableness and effectiveness of the proposed joint bidding method, and the results show that the constructed model overcomes the problem of over-conservatism of the robust model, and the computational adaptability is better than that of the stochastic model, which achieves a better balance between robustness and economy.

KEYWORDS

user-side resource, auxiliary service for peak load balancing, distributionally robust chance constraints, fuzzy set, robustness and economic balance

1 Introduction

Proposals for "carbon peak and carbon neutrality" have promoted the use of new energy sources, such as wind power, as the main power source in new power systems of the future (Xie et al., 2023). However, the integration of large-scale new energy sources into the grid has resulted in serious challenges to the flexible peaking of the power grid (Hasan et al., 2023). In addition, the proportion of traditional regulation resources, such as thermal power, in the grid is decreasing gradually such that it has become difficult to meet system demands by relying only on traditional regulation resources (Li et al., 2023a). Given the continuous improvements in user-side automation, user-side distributed energy storage and other adjustable resources have gradually become a new type of flexible resource to alleviate the pressure of power system peaking (Zhang et al., 2022). User-side adjustable resources not only respond to the demands of grid peak shaving and valley filling but also provide diversified services such as electrical energy, peak shifting, and improvement of new energy consumption through their flexible and adjustable characteristics (Lin et al., 2023).

At present, experts and scholars have conducted numerous studies on the participation of customer-side adjustable resources in electricity market transactions. Khodadadi et al. (2022) proposed bidding and auctioning strategies for flexible load aggregators to participate in the day-ahead and real-time markets, in addition to using stochastic scenarios and robust optimization methods to study the uncertainties in electricity prices and new energy sources, respectively. Bai et al. (2023) noted that customer-side adjustable resources not only participate in the electrical energy market to promote new energy consumption but also provide peaking auxiliary services as flexible interactive resources.

At present, some regions in China, such as North China, Shanghai, and Central China, have issued trading rules for the participation of user-side resources in the peaking market, thus encouraging the participation of user-side resources in flexible peaking through a market-based approach (Cao and Zhang, 2023). Datta and Das (2023) proposed an optimal peak shifting bidding strategy for charging operators by considering the adjustable characteristics of different types of charging stations, with the optimization objectives of minimizing the net operating costs as well as allocation errors. Zhang and Liu (2023) designed a trading strategy for a virtual power plant (VPP) to participate in the peaking market based on the regional trading mechanism in North China. VPP is a special kind of load integrator that can aggregate distributed energy sources, especially energy storage and distributed power sources, to participate in market trading (Alahyari et al., 2019).

Among the power spot pilot units, Gansu, Northeast, Shanxi, and other regions in China are exploring methods to jointly optimize the operations of the peaking auxiliary service and power spot markets (Guo et al., 2020). For example, Shanxi Power Grid now has a preliminary mechanism for integrating the peaking auxiliary service with the spot market and has carried out a settlement trial run (Qin et al., 2023). Customer-side resources often interact with each other when participating in energy trading and flexible peaking auxiliary services, based on which the bidding strategies for their simultaneous participation in both the energy and peaking markets needs to be investigated (Khorasany et al., 2022). A few studies have explored this issue; for example, Li et al. (2023b) investigated a joint trading strategy for VPP participation in the electrical energy and peaking markets, where the VPP participates in peak shaving and peak filling through distributed energy storage and flexible loads. However, this approach ignores the impacts of user-side adjustable resource uncertainties on the decision-making behaviors of the VPPs. Alabi et al. (2021) and Mei et al. (2023) explored VPP participation in direct power trading and flexible peaking operation modes. Here, Alabi et al. (2021) describe the tariffs and new energy output uncertainties using stochastic and robust optimization methods, respectively. Mei et al. (2023) proposed a VPP day-ahead bidding strategy based on the conditional value-at-risk theory by considering wind power uncertainties. Customer-side adjustable resources include not only new energy but also several temperature-controlled loads, electric vehicles, and other adjustable loads (Cheng et al., 2023). Owing to multiple uncertainties such as market tariffs, environment, and customer participation willingness, the actual and predicted customer-side regulation capacities may have large deviations, and the bidding strategies must consider the revenue expectations under these deviated responses; however, none of the above works have considered the impacts of uncertainty of customer-side regulation capacity on the bidding strategy.

Current optimization methods for handling user-side regulation capacity uncertainties mainly include stochastic optimization (SO) and robust optimization (RO), among others. SO generally entails scenario generation through a probability distribution function, which ensures that the random variables satisfy the set constraints in each scenario, such as maximum or minimum response capacity limits (Sarfarazi et al., 2023).

Roald et al. (2023) assumed that the actual regulation capacities of incentive-based demand–response loads obey a truncated normal distribution, and they used a scenario-based SO approach to analyze the impact of user-side regulation capacity uncertainty on the economic dispatch of the system. Chassin and Rondeau (2016) proposed an electric energy market bidding strategy that takes into account the demand–response load uncertainty by assuming that the residential demand–response load participation rates obey normal, uniform, and skewed distributions. The performance of an SO method is determined by the accuracy of the probability distribution function of uncertain variables. However, given the diverse types of customer-side resources and large differences in their uncertainty characteristics, it is difficult to accurately describe the probability distribution of the actual regulation capacities of different types of customer-side resources. RO generally describes the range of variation of user-side response capacity through the uncertainty set and makes decisions based on the worst-case scenario (Li et al., 2023c). Du et al. (2024) investigated the demand–response load uncertainty based on real-time tariffs using an RO approach. The difficulty of RO lies in the construction of a suitable uncertainty set, and the commonly used uncertainty sets are the box, polyhedron, and ellipsoid sets, among others (Zhang et al., 2023). The customer-side regulation capacity uncertainty is related to multiple factors, such as the load participation rate, load type, and weather, while the uncertainty set is difficult to determine, leading to overly conservative results and lack of economy if the RO method is used directly.

In recent years, the distributionally robust chance constrained (DRCC) optimization method has garnered attention as it neither assumes a probability distribution function nor completely ignores information on probability distributions (Schwidtal et al., 2023). The DRCC model is based on a data-driven approach to construct a fuzzy set containing all possible probability distributions that is then solved on the basis of the worst probability distribution fuzzy set and worst-case probability distribution (Al-Jabouri et al., 2024). Compared with SO and chance constraints, the DRCC model does not assume that the uncertain variables obey specific probability distributions, which is more robust; compared with RO, the DRCC method considers all possible probability distribution data, which is less conservative (Liang et al., 2023). At present, DRCC methods have been studied for unit combination and economic dispatch; it is mostly used to handle the uncertainties of wind power, photovoltaic output, and load demand (Pan et al., 2023). There are very few studies on the application of the DRCC method to solve the bidding decision problem by considering uncertainty. For example, Jin et al. (2023) used the DRCC method to describe electric vehicle regulation capability uncertainty and proposed a bid-allocation decision method for electric vehicle aggregators. However, there are not many studies on applying the DRCC method to cope with user-side regulation capacity uncertainty in the user-side bidding decision problem. The use of the DRCC approach to handle user-side response uncertainty enables characterization of not only the uncertainty features of multiple types of user-side resources but also the variability of the uncertainty features. The constructed data-driven fuzzy set based on DRCC covers the uncertainty features of different types of loads and can solve the multitype user-side regulation capacity uncertainty problem more effectively.

This paper presents an integrated study of the joint optimization bidding strategy for user-side resources in both the day-ahead energy market and peaking ancillary services market. Initially, the DRCC method is used to establish an uncertainty model for user-side regulation capacity. In addressing the issue of diverse user-side resource types with significant differences in the uncertainty characteristics, which cannot be accurately described with a precise probability density function, this study employs a data-driven approach to construct fuzzy sets that characterize the load uncertainties without assuming a specific probability distribution for the random variables. Subsequently, to tackle the bidding risks arising from the user-side regulation capacity uncertainty, a risk-aware trading decision-making method is proposed that incorporates risk expectations and opportunity constraints. This method transforms the problem into a linear programming problem by applying a strong duality theory with a conditional value approximation method that can be solved using a commercial solver. Finally, the effectiveness of the risk-based bidding strategy grounded in the DRCC model is validated through numerical simulation.

2 User-side load modeling

Loads can participate in market transactions through tariff-based demand–response; they can independently choose the time to participate in regulation and the corresponding regulation capacity based on the tariff signal. Given the uncertainties in the response behaviors of different types of loads at different tariff levels, there are large deviations between the regulation capacities of the loads, i.e., the actual regulation capacity available for participating in the market and predicted value, which in turn pose revenue risks to the design of customer-side bidding strategies. Accordingly, the uncertainty in customer-side regulation capacity is modeled first. Section 2.1 provides an overview of the load deterministic model to measure the regulation capacities of loads participating in the market bidding, and Section 2.2 portrays the load regulation capacity uncertainty characteristics using the data-driven DRCC approach.

2.1 Load deterministic modeling

Tariff-based demand–response shifts the load demand by differentiating the purchase price of electricity, e.g., by increasing the price of electricity during peak hours and lowering it in the trough, thereby achieving peak shaving, valley filling, and smoothing of the load curve. The sensitivity of a load to changes in the electricity price is generally described by the elasticity coefficient. To reflect the sensitivities of different types of loads to price changes, we model the uncertainties of the user-side resources through the opportunity constraints of the SemBleu samples and construct the load deterministic model using the dynamic elastic coefficient to represent the variation in electricity prices during different periods. Assuming that the load demand P_i is linearly related to the price ρ_i ($P_i = -a_i\rho_i + b_i$), the dynamic elasticity coefficient can be expressed as

$$E_{ii} = \frac{-a_i\rho_i}{-a_i\rho_i + b_i} \tag{1}$$

$$E_{ij} = \frac{-2a_i^2\rho_j + a_ib_i}{\left\{b_i^2 + 4\left[-a_i^2\left(\rho_j^2 + \rho_k^2\right) + a_ib_i\left(\rho_j + \rho_k\right) - a_iI + \sum_{\substack{L=1 \\ L\neq i,j}}^{N} - a_i^2\rho_L^2 + a_ib_i\rho_L\right]\right\}^{1/2}} * \frac{\rho_j}{-a_i\rho_j + b_i} \quad L = 1\ldots, i\ldots, j\ldots, N, \tag{2}$$

where in Equations (1, 2), E_{ii} denotes the dynamic self-elasticity coefficient for a single time response, i.e., the load change is only related to the price at that time, and is generally set to a value less than or equal to 0. E_{ij} denotes the dynamic cross-elasticity coefficient for the multitime response, i.e., the price change in one time period causes load changes in other periods, and is generally set to a value greater than 0. ρ_j and ρ_k denote the tariffs at the corresponding moments, a_i and b_i denote the demand function parameters, I denotes the cost of purchasing electricity for the load, and N denotes the number of tariff-based demand–response items.

Based on the dynamic elasticity factor, the load regulation capacity is expressed as

$$P_i^{DR} = \eta\rho_{0,i}\left\{E_{i,i}\frac{\rho_i - \rho_{0,i}}{\rho_{0,i}}\sum_{\substack{j=1 \\ i\neq j}}^{24} E_{i,j}\frac{\rho_j - \rho_{o,j}}{\rho_{o,j}}\right\}, \tag{3}$$

$$\rho_{\min} \le \rho_i \le \rho_{\max}, \tag{4}$$

$$P_{\min}^{\mathrm{DR}} \le P_i^{\mathrm{DR}} \le P_{\max}^{\mathrm{DR}}, \tag{5}$$

where $P_{0,i}$ and P_i^{DR} denote the load demand and load regulation capacity before participating in demand–response, respectively; η denotes the participation rate that ranges from 0 to 1—the larger this value, the higher is the possibility that the load is willing to participate in the demand–response program; $\rho_{0,i}$ and $\rho_{0,j}$ denote the prices of electricity at the corresponding moments before participation in the demand–response program; $\rho_{\max}$ and $\rho_{0,j}$ denote the upper and lower limits of the power purchase price and are given by the trading center to ensure reasonable price levels; $P_{\max}^{\mathrm{DR}}$ and $P_{\min}^{\mathrm{DR}}$ denote the maximum and minimum allowed regulation capacities, respectively.

2.2 Load regulation capacity uncertainty modeling

Based on the deterministic model given in Equations (3–5), the uncertainty model based on the DRCC method is explored herein.

Considering that the load regulation capacity is related to multiple influencing factors, such as user participation rate and price, the regulation capacity is difficult to accurately predict in reality; hence, the actual regulation capacity of the load is expressed as

$$\tilde{P}^{\mathrm{DR}} = P^{\mathrm{DR}} + \xi^{\mathrm{DR}}, \tag{6}$$

where in Equation (6), $\tilde{P}^{\mathrm{DR}}$ is the form of uncertainty in the regulation capacity, and ξ^{DR} denotes the prediction error.

There are various types of loads, including industrial loads (e.g., steel industry) and residential loads (e.g., electric vehicles). In practice, it is difficult to accurately describe the specific probability distribution of the load prediction errors owing to the stochastic nature of their response behaviors and differing sensitivities of different types of loads to different influencing factors. To address this issue, we use a data-driven DRCC model to regulate the capacity uncertainties of multiple types of loads. The basic idea of this method is to construct a fuzzy uncertainty set containing all possible probability distributions based on historical data to describe the load regulation capacity differentiation uncertainty. The method not only utilizes the probability distribution information characterized by real historical data of the loads fully but also avoids the arbitrariness of setting a particular probability distribution directly.

2.2.1 Fuzzy sets based on Wasserstein distance

The Equation (7) based on the historical load-regulated capacity data, the set of samples of N groups $\left\{\tilde{\xi}_1, \tilde{\xi}_2, \ldots, \tilde{\xi}_N\right\}$ is selected randomly with probability distributions $\{P_1, P_2, \ldots, P_N\}$, respectively; the probability distribution of the mean of the samples ξ_μ is used as the empirical distribution P_N of the load prediction error $\tilde{\xi}^{\mathrm{DR}}$ as well as estimate of the true distribution P:

$$\xi_\mu = \frac{1}{N}\sum_{n\in N} \tilde{\xi}_n. \tag{7}$$

The probability distance between the empirical and true distributions, i.e., the Wasserstein distance can be expressed as

$$W(P_N, P) = \inf\left\{\int d\left(\xi_\mu, \xi_t\right)\prod\left(d\xi_\mu, d\xi_t\right)\right\}, \tag{8}$$

$$d\left(\xi_\mu, \xi_t\right) = \left\|\xi_\mu - \xi_t\right\|, \tag{9}$$

where in Equations (8, 9), ξ_μ and ξ_t denote the load prediction errors obeying the empirical distribution P_N and true distribution P, respectively; $d(\xi_\mu, \xi_t)$ represents the Euclidean norm between ξ_μ and ξ_t; $\prod(d\xi_\mu, d\xi_t)$ denotes the joint distribution of P_N and P; inf is the lower bound function.

A spherical fuzzy set D_0 was built with the empirical distribution of load forecasting errors centered on the Wasserstein probability distance as the radius:

$$D_0 = \left\{P_i \in M(\Xi) \,\middle|\, W(P_N, P) \le \rho\right\}, \tag{10}$$

where in Equation (10), $M(\Xi)$ is the set of all probability distributions on the uncertainty set Ξ; M represents the fuzzy set centered on the empirical distribution of the load forecasting error P_N with radius ρ, which contains all possible probability distributions, including the empirical distribution of load forecasting error with a certain level of confidence. ρ can be obtained by a dichotomous search based on the sample data.

2.2.2 Uncertainty sets based on the data-driven approach

In practical scenarios, the uncertainty set is constructed by analyzing the boundaries of the load forecast error; first, the sample set of historical data is normalized as

$$\tilde{\theta}_n = \tilde{\Sigma}^{-\frac{1}{2}}\left(\tilde{\xi}_n - \tilde{\mu}\right), n = 1, 2, \ldots, N, \tag{11}$$

where in Equation (11), $\tilde{\mu}$ and $\tilde{\Sigma}$ denote the sample mean and variance, respectively. The uncertain set $\tilde{\theta}$ of Ξ is then expressed as

$$\Xi = \left\{\tilde{\theta} \in R^N \,\middle|\, -l \le \tilde{\theta}^i \le l\right\} \tag{12}$$

where in Equation (12), l denotes the restricted range of the parameter $\tilde{\theta}$. According to Fan et al. (2023a), we have

$$\begin{cases} \min\limits_{l < l_{\max}} l \\ \text{s.t.} \sup\limits_{\mathrm{P}^{\mathrm{std}} \in P^{\mathrm{std}}} \mathrm{P}^{\mathrm{std}}\left(\tilde{\theta} \notin \Xi\right) \le 1 - \eta, \end{cases} \tag{13}$$

where p^{std} and P^{std} denote the probability distribution and fuzzy set of $\tilde{\theta}$; η is the confidence level of the uncertainty set. Based on dyadic theory, Equation (13) can be transformed into Equation (14), which is then solved with the nested dichotomy method:

$$\begin{cases} \min\limits_{l < l_{\max}} l \\ \text{s.t.} \left\{\kappa \cdot \varepsilon + \dfrac{1}{N}\sum\limits_{n=1}^{N}\left(1 - \kappa\left(l - \left\|\tilde{\theta}_n\right\|\right)^+\right)^+\right\} \le 1 - \eta, \\ \kappa \ge 0 \end{cases} \tag{14}$$

where $(\cdot)^+ = \max(\cdot, 0)$, κ, ε denote the dyadic variables in the transformation process.

3 Modeling of joint bidding for user-side participation in the electrical energy and peaking ancillary services markets

This section presents the construction of a joint bidding decision optimization model for customer-side participation in the day-ahead electrical energy and peaking ancillary services markets to improve the market returns from customer-side resources. First, we construct a user-side preparticipation market deterministic bidding model and study the relevant constraints. Then, we construct a user-side preparticipation market risk bidding model by accounting for uncertainty and the risk bidding strategy of user-side participation in the joint market. The model effectively handles the uncertainty of user-side resources and reflects the changes in the user-side returns by adjusting the risk parameters and confidence levels.

3.1 Deterministic bidding model for the market before the day of user-side participation

3.1.1 Objective function

Customer-side resources, including distributed generation resources, distributed energy storage, and demand–response loads, can gain revenue by participating in the electrical energy and peaking ancillary services markets; however, they also have to bear the costs for purchasing electricity from the grid and operations. In this work, the optimization objective is to minimize the bidding cost for the user side to participate in the joint market a few days prior, and the bidding cost F includes the cost of purchasing and selling electricity in the energy market C_e, operating cost for distributed energy storage C_{ES}, and peak shifting revenue B_f. These details are summarized in Equation (15):

$$F = \min\left(C_e + C_{ES} - B_f\right). \tag{15}$$

The cost for participating in electricity purchase and sale transactions in the electricity energy market C_e is given by

$$C_e = \sum_t \left(\rho_t^b P_t^b - \rho_t^s P_t^s\right)\Delta t, \tag{16}$$

where in Equation (16), ρ_t^b and ρ_t^s, respectively, denote the prices of electricity purchased and sold during time slot t; P_t^b and P_t^s, respectively, denote the capacities purchased and sold during time slot t; Δt denotes the time interval, which is set as 1 h in this study.

The operating cost for distributed energy storage C_{ES} is given by

$$C_{ES} = \sum_t \sum_i c_{ch,i}\left(P_{ch,i,t}^{ES} + P_{i,t}^{ES,vf}\right)\Delta t + c_{dis,i}\left(P_{dis,i,t}^{ES} + P_{i,t}^{ES,pf}\right)\Delta t. \tag{17}$$

where in Equation (17), $c_{ch,i}$ and $c_{dis,i}$ represent the respective unit charging and discharging costs of the energy storage at i; $P_{ch,i,t}^{ES}$ and $P_{dis,i,t}^{ES}$ represent the corresponding charging and discharging capacities of the energy storage at t; $P_{i,t}^{ES,vf}$ and $P_{i,t}^{ES,pf}$ denote the participation of energy storage in peak filling and peak shaving power at time period t, respectively.

The peak shifting revenue B_f is given by

$$B_f = \sum_t \left(\rho_{pf} P_t^{pf} + \rho_{vf} P_t^{vf}\right)\Delta t, \tag{18}$$

$$P_t^{pf} = P_t^{REN,pf} + \sum_{i=1}^{N^{ES}} P_{i,t}^{ES,pf} + \sum_{j=1}^{N^{DR}} P_{j,t}^{DR,pf}, \tag{19}$$

$$P_t^{vf} = P_t^{REN,vf} + \sum_{i=1}^{N^{ES}} P_{i,t}^{ES,vf} + \sum_{j=1}^{N^{DR}} P_{j,t}^{DR,vf}, \tag{20}$$

where in Equations (18)–(20), ρ_{pf} and ρ_{vf} denote the compensation prices of auxiliary services for peak shaving and valley filling, respectively; $P_t^{DR,pf}$ and $P_t^{DR,vf}$ denote the peak shaving and peak filling bidding capacities submitted for time t, respectively; $P_t^{REN,pf}$ and $P_t^{REN,vf}$ denote the downward and upward capacities of new energy resources participating in peak shaving and valley filling, respectively; N^{ES} and N^{DR} denote the number of distributed storage and demand–response loads, respectively; $P_{i,t}^{ES,pf}$ and $P_{i,t}^{ES,vf}$ denote the number of discharges of distributed storage units participating in peak shaving and the charging amount of valley filling, respectively; $P_{j,t}^{DR,pf}$ and $P_{j,t}^{DR,vf}$ denote the amount of reduction in loads participating in peak shaving and increase in loads participating in valley filling, respectively.

3.1.2 Constraints

The constraints are formulated using the internal power and bid capacity limits for new energy and storage.

The following constraints need to be met for the user side to participate in the joint market trading of day-ahead energy and peaking ancillary services:

3.1.2.1 Internal power balance constraints

$$P_t^b - P_t^s = D_t - \sum_{i=1}^{N^{ES}} P_{i,t}^{ES} - \sum_{j=1}^{N^{DR}} P_{j,t}^{DR} - P_t^{REN}, \tag{21}$$

where in Equation (21), D_t denotes the power demand during time t before the load participates in demand–response; P_t^{REN} and $P_{i,t}^{ES}$ denote the total bidding capacities of new energy and energy storage participating in the joint market, respectively.

3.1.2.2 New energy bidding constraints

$$P_t^{REN,e} + P_t^{REN,pf} \le P_t^{REN,max}, \tag{22}$$

$$P_t^{REN,e} - P_t^{REN,vf} \ge 0, \tag{23}$$

where Equations (22, 23) represent the bidding capacity constraints for new energy to participate in both the electrical energy and peaking ancillary services markets, i.e., the upward change of the new energy is no more than the maximum projected output on a generation basis and the downward change is no less than 0.

3.1.2.3 Distributed energy storage bidding constraints

$$0 \le P_{ch,i,t}^{ES}, P_{dis,i,t}^{ES} \le P_{i,max}^{ES}. \tag{24}$$

$$P_{i,t}^{ES,e} = P_{dis,i,t}^{ES} - P_{ch,i,t}^{ES}. \tag{25}$$

$$P_{i,t}^{\mathrm{ES,e}} + P_{i,t}^{\mathrm{ES,pf}} \le P_{i,\max}^{\mathrm{ES}}. \tag{26}$$

$$P_{i,t}^{\mathrm{ES,e}} - P_{i,t}^{\mathrm{ES,vf}} \ge -P_{i,\max}^{\mathrm{ES}}. \tag{27}$$

$$E_{i,t} = E_{i,t-1} + P_{\mathrm{ch},i,t}^{\mathrm{ES}}\eta_{\mathrm{c}}\Delta t - \frac{P_{\mathrm{dis},i,t}^{\mathrm{ES}}}{\eta_{\mathrm{d}}\Delta t} + P_{\mathrm{vf},i,t}^{\mathrm{ES}}\eta_{\mathrm{c}}\Delta t - \frac{P_{\mathrm{pf},i,t}^{\mathrm{ES}}}{\eta_{\mathrm{d}}\Delta t}. \tag{28}$$

$$E_{\min} \le E_{i,t} \le E_{\max}. \tag{29}$$

$$E_{i,t_0} = E_{i,T}. \tag{30}$$

Here, Equation (24) represents the charging and discharging power limitation constraints for distributed energy storage, and $P_{i,\max}$ represents the maximum charging and discharging power; Equation (25) represents the bidding capacity of distributed energy storage for participation in the electrical energy market, where $P_{i,t}^{\mathrm{ES,e}}$ is equal to the difference between the charging and discharging power. Equations (26, 27) represent the bidding capacity constraints of distributed energy storage for participation in the joint electrical energy and peaking markets; Equation (28) represents the energy balance constraints of distributed energy storage, where E_t and E_{t-1} represent the storage energies at t and $t-1$, respectively. Equation (29) represents the storage energy constraints, where $E_{\max}$ and $E_{\min}$ represent the maximum and minimum storage energy limitations, respectively. In Equation (30), E_{i,t_0} and $E_{i,T}$ represent the energy at the initial and end moments of energy storage, respectively. The energy storage has two states as charging and discharging, and the 0–1 values representing the charging and discharging states should be added to the operating constraints of Equation (24) while considering the logical constraints, i.e., to avoid charging and discharging the energy storage at the same time. However, considering that the operating constraints of the energy storage will be applied to the objective function to solve the minimum transaction cost of the integrator, if the charging and discharging behaviors of the energy storage occur at the same time, some of the effective values will be canceled out at the corresponding moments, and the optimal solution cannot be derived; therefore, the 0–1 values and logical constraints are not added in the optimization model of the energy storage in this work, which will help speed up the solution and reduce the running time.

3.1.2.4 Demand–response load bidding constraints

$$-P_{i,\max}^{\mathrm{DR}} \le P_{i,t}^{\mathrm{DR,e}} \le P_{i,\max}^{\mathrm{DR}}. \tag{31}$$

$$0 \le P_{i,t}^{\mathrm{DR,pf}} \le U_{i,t}^{\mathrm{pf}} P_{i,\max}^{\mathrm{DR}}. \tag{32}$$

$$0 \le P_{i,t}^{\mathrm{DR,vf}} \le U_{i,t}^{\mathrm{vf}} P_{i,\max}^{\mathrm{DR}}. \tag{33}$$

$$U_{i,t}^{\mathrm{vf}} + U_{i,t}^{\mathrm{pf}} \le 1. \tag{34}$$

$$P_{i,t}^{\mathrm{DR,e}} + P_{i,t}^{\mathrm{DR,pf}} \le P_{i,\max}^{\mathrm{DR}}. \tag{35}$$

$$P_{i,t}^{\mathrm{DR,e}} - P_{i,t}^{\mathrm{DR,vf}} \ge -P_{i,\max}^{\mathrm{DR}}. \tag{36}$$

Here, Equation (31) indicates that the demand–response load i participates in the bidding capacity constraint of the electrical energy market, and $P_{i,\max}^{\mathrm{DR}}$ is the maximum adjustment capacity allowed for the demand–response load on the day before. Equations (32, 33) indicate that the demand–response load participates in the bidding capacity constraints for peak shaving and valley filling, and $U_{i,t}^{\mathrm{pf}}$ and $U_{i,t}^{\mathrm{vf}}$ indicate the states for participating in peak shaving and valley filling, respectively, with the value 1 indicating participation. Equation (34) indicates that the load cannot participate in peak shaving and valley filling at the same time, while Equations (35, 36) indicate that the demand–response load participates in the bidding capacity constraint of the joint market.

3.2 Market risk bidding model for day-ahead markets taking uncertainty into account

Based on the previous analysis, load uncertainty poses a revenue risk to decision-makers when formulating bidding strategies. To address this problem, we constructed a risky bidding decision model for user-side participation in the day-ahead market based on the distributional robust opportunity constrained optimization method. To construct the user-side day-ahead market risk bidding model that accounts for uncertainty, we first reconstructed the objective function by considering risk expectation and then analyzed the uncertainty of load capacity regulation with opportunity constraints to build the model.

3.2.1 Objective function reconstruction considering risk expectations

The load uncertainty variable error is set to ξ^{DR}, such that the load $\tilde{P}_{i,t}^{\mathrm{DR}}$ containing the uncertainty variable can be expressed as

$$\tilde{P}_{i,t}^{\mathrm{DR}} = P_{i,t}^{\mathrm{DR}} + \xi_{i,t}^{\mathrm{DR}}. \tag{37}$$

By substituting Equation (37) into the objective function of Equation (15), we get Equation (38):

$$\min C = \min \sum_{\mathrm{t}=1}^{\mathrm{T}} \left(C_{\mathrm{e}} + C_{\mathrm{ES}} - \tilde{B}_{\mathrm{f}}\right). \tag{38}$$

The objective function of the risky bidding decision model is as shown in Equation (39) and consists of two components: the bidding cost of participating in the joint market and the expected cost of coping with the risks associated with uncertainty.

$$\min \sum_{t=1}^{\mathrm{T}} (C_{\mathrm{e}} + C_{\mathrm{ES}} - B_{\mathrm{f}}) + \min \max_{P \in D_0} E_P C\left(\xi^{\mathrm{DR}}\right), \tag{39}$$

where E_P denotes the expected probability.

For convenience, the objective function of the DRCC model is written in the following abstract form:

$$\min_{x} a^{\mathrm{T}} x + \min_{x} \max_{P \in D_0} E_P\{b^{\mathrm{T}}\xi\}, \tag{40}$$

where in Equation (40), x represents the decision variable, ξ represents the uncertainty variable, and a^{T} and b^{T} are the corresponding coefficients.

3.2.2 Opportunity constraint construction

Owing to uncertainty in the load regulation capacity, the bidding process for load participation in the joint electricity markets (i.e., electrical energy, peak shaving and peaking, and valley filling and peaking markets) has the same uncertainty. We introduce chance constraints to handle optimization problems containing random variables and increase the model robustness by setting a confidence level that allows the constraints to remain unsatisfied under a certain probability. There is also uncertainty in the capacity for handling load regulation. Specifically, this work uses

opportunity constraints to model and analyze these uncertainties, as shown in Equations (41–45):

$$\inf_{P\in D_0} E_P\left(-P^{\mathrm{DR}}_{i,\max} \le P^{\mathrm{DR,e}}_{i,t} + \xi^{\mathrm{DR,e}} \le P^{\mathrm{DR}}_{i,\max}\right) \ge 1-\varepsilon. \tag{41}$$

$$\inf_{P\in D_0} E_P\left(0 \le P^{\mathrm{DR,pf}}_{i,t} + \xi^{\mathrm{DR,pf}} \le U^{\mathrm{pf}}_{i,t} P^{\mathrm{DR}}_{i,\max}\right) \ge 1-\varepsilon. \tag{42}$$

$$\inf_{P\in D_0} E_P\left(0 \le P^{\mathrm{DR,vf}}_{i,t} + \xi^{\mathrm{DR,vf}} \le U^{\mathrm{vf}}_{i,t} P^{\mathrm{DR}}_{i,\max}\right) \ge 1-\varepsilon. \tag{43}$$

$$\inf_{P\in D_0} E_P\left(P^{\mathrm{DR,e}}_{i,t} + P^{\mathrm{DR,pf}}_{i,t} + \xi^{\mathrm{DR,e}} + \xi^{\mathrm{DR,pf}} \le P^{\mathrm{DR}}_{i,\max}\right) \ge 1-\varepsilon. \tag{44}$$

$$\inf_{P\in D_0} E_P\left(P^{\mathrm{DR,e}}_{i,t} - P^{\mathrm{DR,vf}}_{i,t} + \xi^{\mathrm{DR,e}} + \xi^{\mathrm{DR,vf}} \ge -P^{\mathrm{DR}}_{i,\max}\right) \ge 1-\varepsilon. \tag{45}$$

Here, Equations (41–45) denote the load bidding opportunity constraints for the electrical energy, peak shaving, and peak filling markets that are guaranteed to fail in the fuzzy set D_0 space with probability E_P less than the set confidence level ε, where ε denotes the risk probability of the load bidding constraints overstepping the limit. $\xi^{\mathrm{DR,e}}$, $\xi^{\mathrm{DR,pf}}$, and $\xi^{\mathrm{DR,vf}}$ are the load forecast errors of the electrical energy, peak shaving, and peak filling markets, respectively.

4 Model solution

In the DRCC model considering risk expectation, the objective function contains a min–max two-layer structure and non-linear chance constraints that make it difficult to solve directly. First, we transformed the inner max problem of the model into a min problem based on the strong duality theory and then transformed the two-layer optimization to a single-layer optimization problem before solving the model using the fuzzy uncertainty set of load regulation capacity.

4.1 Objective function pairwise transformation

The objective function of the risk expectation DRCC model contains a min–max two-layer structure, which makes it difficult to solve directly. According to Slater's theorem, the strong duality theory describes a special relationship between the primal and duality problems; if the primal and duality problems both have feasible solutions, then as long as one problem has an optimal solution, the other problem must also have an optimal solution, where the objective function values of the two optimal solutions are equal. Conditional value at risk refers to the average loss of the portfolio under the condition that this loss exceeds a given VaR value; it is known that the strong duality of the model holds, so we transformed the inner max problem to a min problem using the strong duality theory; further, we transformed the double-layer optimization to a single-layer optimization problem. The specific process is as follows:

$$\begin{aligned}
&\min_x a^{\mathrm{T}}x + \min_x \max_{P\in D_0} E_P\{b^{\mathrm{T}}\xi\} \\
&= \begin{cases} \min\limits_{\lambda^0, s_i^0} a^{\mathrm{T}}x + \lambda^0\rho + \dfrac{1}{N}\sum\limits_{i=1}^{N} s_i^0 \\ s.t. \begin{cases} \min\limits_{\|z_n\|_*\le\lambda^0} \max\limits_{\xi\in\Xi}\left[b^{\mathrm{T}}\xi - z_i^{\mathrm{T}}(\xi-\xi_i)\right] \le s_i^0 \\ \|z_i\|_* \le \lambda^0, \forall i \in N \end{cases} \end{cases},
\end{aligned} \tag{46}$$

where the random variable ξ denotes $\xi^{\mathrm{DR}}_{i,t}$; $a^T x$ denotes the bid cost in the deterministic model $C_{\mathrm{e}} + C_{\mathrm{ES}} - B_{\mathrm{f}}$; $b^{\mathrm{T}}\xi$ is equal to $\rho_{\mathrm{pf}} u^{\mathrm{pf}} \xi^{\mathrm{DR}}_{i,t} + \rho_{\mathrm{vf}} u^{\mathrm{vf}} \xi^{\mathrm{DR}}_{i,t}$; λ^0, s_i^0, and z_i^{T} denote the dyadic factors in the transformation process; $\|\|_*$ denotes the dyadic paradigm.

According to the fuzzy uncertainty set of the load regulation capacity constructed in Section 2.2, the specific expression of the probability distribution space Ξ is

$$\begin{cases} \Xi = \{H\xi \le h\} \\ H = [I, -I]^{\mathrm{T}} \\ h = [l, -l] \end{cases}, \tag{47}$$

where H and h denote the coefficient matrix and right-end vector of the polyhedron, respectively.

The constraint inner layer function in Equation (46) can only take its maximum value at the boundary of the load uncertainty set, which can be obtained by substituting Equation (47) into Equation (46):

$$\begin{aligned}
&\min_{\|z_i\|_*\le\lambda^0} \max_{\Xi=\{\xi \mid H\xi\le h\}} \left[b^{\mathrm{T}}\xi - z_i^{T}(\xi-\xi_i)\right] \\
&= \min_{\|z_i\|_*\le\lambda^0} \min_{\gamma_i^0\in\left\{\gamma_i^0 \mid H^{\mathrm{T}}\gamma_i^0 = b^{\mathrm{T}} - z_i\right\}} \left[h^{\mathrm{T}}\gamma_i^0 + z_i^{\mathrm{T}}\xi_i\right],
\end{aligned} \tag{48}$$

where in Equation (48), γ_i^0 denotes the decision variable.

In summary, considering the risk expectation DRCC model, the objective function can be pairwise transformed into a single-layer optimization model, as shown in Equation (49):

$$\begin{aligned}
&\min_{\lambda^0, s_i^0} a^{\mathrm{T}}\mathrm{x} + \lambda^0\rho + \frac{1}{N}\sum_{i=1}^{N} s_i^0 \\
&s.t. \begin{cases} b^{\mathrm{T}}\xi_i + \gamma_i^0(h - H\xi_i) \le s_i^0. \\ \left\|H^{\mathrm{T}}\gamma_i^0 - b^{\mathrm{T}}\right\|_* \le \lambda^0 \\ \gamma_i^0 \ge 0, \forall i \in N \end{cases}
\end{aligned} \tag{49}$$

Then, the objective function is transformed into the expression of Equation (50) as Equation (55):

$$\begin{aligned}
&\min_{\lambda^0, s_i^0} C_{\mathrm{e}} + C_{\mathrm{ES}} - B_{\mathrm{f}} + \lambda^0\rho + \frac{1}{N}\sum_{i=1}^{N} s_i^0 \\
&s.t. \begin{cases} \rho_{\mathrm{pf}} u^{\mathrm{pf}} \xi^{\mathrm{dr}}_{i,t} + \rho_{\mathrm{vf}} u^{\mathrm{vf}} \xi^{\mathrm{dr}}_{i,t} + \gamma_i^0 \xi_i \le s_i^0 \\ -\lambda^0 \le \gamma_i^0 - \rho_{\mathrm{pf}} u^{\mathrm{pf}} - \rho_{\mathrm{vf}} u^{\mathrm{vf}} \le \lambda^0 \\ \gamma_i^0 \ge 0, \forall i \in N \end{cases}.
\end{aligned} \tag{50}$$

4.2 Conditional value-at-risk approximation

The general form of the opportunity constraints in Equations (41–45) of the model can be expressed as

$$\inf_{P\in D_0} E_P\{\alpha_k(x)\xi_i \le \beta_k(x)\} \ge 1-\varepsilon, \tag{51}$$

where k denotes the number of chance constraints, and $\alpha_k(x)$ and $\beta_k(x)$ denote the coefficients of the constraints and right-end vector, respectively.

The opportunity constraints are non-linear inequality constraints and are difficult to solve directly. In this work, the conditional value-at-risk concept is used to approximate the

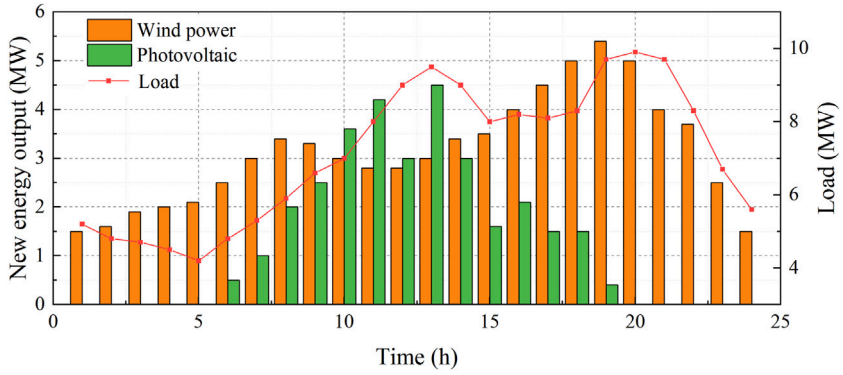

FIGURE 1
Predicted output curves for new energy sources and loads.

opportunity constraints, which are then transformed into a linear programming model for processing. The specific process is as follows.

The chance constraint inequality of Equation (51) can be expressed as

$$\sup_{P\epsilon D_0} E_P - \mathrm{CVaR}_\varepsilon\{\alpha_k(x)\xi_i \le \beta_k(x)\} \le 0. \tag{52}$$

According to Theorem 1 in Ordoudis et al. (2021), the conditional value-at-risk not only considers the potential maximum loss at a given confidence level but also measures the average loss exceeding this threshold. By introducing appropriate variables and constraints, the risk measure of the conditional VaR is transformed to a part of the linear programming model, which is then solved using the standard linear programming technique; thus, Equation (52) can be transformed into the linear constraint given in Equation (53):

$$\begin{cases} \lambda_k\rho + \dfrac{1}{N}\sum_{i=1}^{N} s_{ik} \le 0 \\ \tau_k \le s_{ik} \\ \alpha_k(x)\xi_i - \beta_k(x) + (\varepsilon-1)\tau_k + \varepsilon\gamma_{ik}^{\mathrm{T}}(h - H\xi_i) \le \varepsilon s_{ik}, \\ \left\|\varepsilon H^{\mathrm{T}}\gamma_{ik} - \alpha_k\right\|_* \le \varepsilon\lambda_k \end{cases} \tag{53}$$

where λ_k, s_{ik}, and τ_k denote the dyadic variables in the transformation process, and γ_{ik} denotes the introduced decision variables.

By taking Equation (41) as an example, we have

$$\inf_{P\epsilon D_0} E_P\left(P_{i,t}^{\mathrm{DR,e}} + \xi^{\mathrm{DR,e}} \le P_{i,\max}^{\mathrm{DR}}\right) \ge 1 - \varepsilon. \tag{54}$$

Then, the constraint Equation (54) is transformed into the expression of Equation (53) as Equation (55):

$$\begin{cases} \lambda_k\rho + \dfrac{1}{N}\sum_{i=1}^{N} s_{ik} \le 0 \\ \tau_k \le s_{ik} \\ \xi^{\mathrm{DR,e}} + P_{i,t}^{\mathrm{DR,e}} - P_{i,\max}^{\mathrm{DR}} + (\varepsilon-1)\tau_k + \varepsilon\gamma_{ik}^{\mathrm{T}}\xi_i^{\mathrm{DR,e}} \le \varepsilon s_{ik}. \\ -\varepsilon\lambda_k \le \gamma_{ik}^{\mathrm{T}} - I \le \varepsilon\lambda_k \end{cases} \tag{55}$$

5 Example analysis

5.1 Parameter settings

The customer-side resources mainly include wind power, photovoltaic output, distributed energy storage, and demand–response loads, among which wind power, photovoltaic output, and load demand forecast are as shown in Figure 1. The relevant parameters of the distributed energy storage are shown in Table 1 (Fan et al., 2023b). The maximum adjustment of the demand–response load at each moment in time does not exceed 10% of the base load value. The dynamic elasticity coefficient of the tariff-based demand–response is referred from Tan et al. (2017), and the parameters are set as shown in Figure 2. Load-side participation in the electricity market purchase and sale of the peak and valley prices of the electricity transactions for each time period are shown in Table 2. The peaking market peak filling, peak shaving/peaking time division, and tariffs are shown in Table 3. Our parameters are set on the basis of the forecast outputs of distributed energy storage and demand–response load mentioned in literature, while utilizing the relevant electricity price data published by the grid company.

5.2 Analysis of optimized bidding decisions in the previous day's market

To verify the effectiveness of the bidding model constructed herein, the following four scenarios are established for comparative analysis. The purpose of Scenario 1 is to establish a baseline case that does not consider the uncertainty of user-side adjustment capacity; based on Scenario 1, Scenario 2 additionally includes the case that the user-side participates in the auxiliary service market for peak regulation at the same time. Scenario 3 focuses on user-side resources when only participating in the electricity market bidding, and the uncertainty of user-side regulation capacity is considered. Scenario 4 entails simulating the operating environment closest to the actual scenario and evaluates the effectiveness and robustness of the proposed strategy under dual uncertainty from market and regulatory capacities.

TABLE 1 Parameters of distributed energy storage.

Rated capacity (MWh)	Rated charge/discharge power (MW)	Charge state range	Initial charge state	Charge and discharge efficiency
5	1	0.1–0.9	0.2	0.95

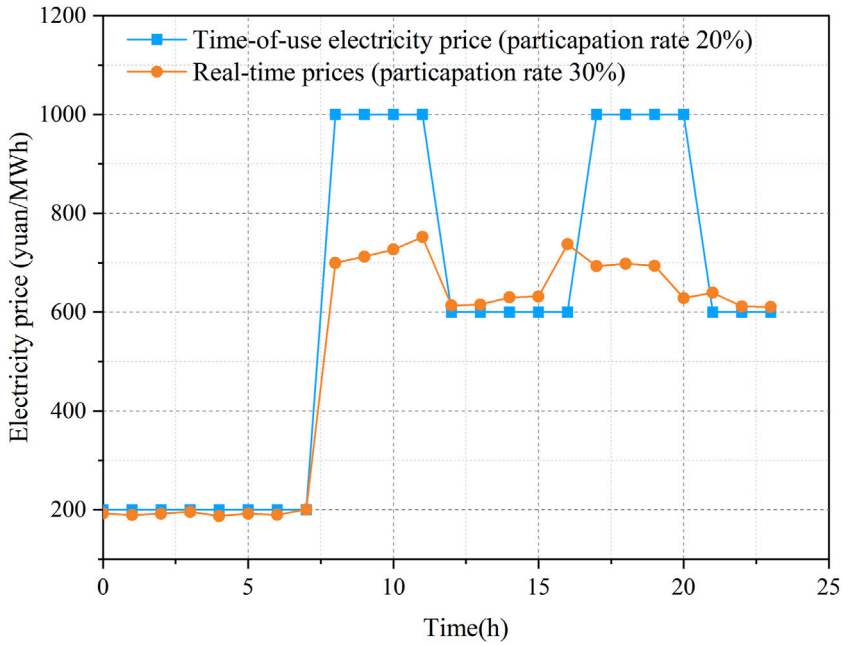

FIGURE 2
Electricity-pricing-based load-related parameters.

TABLE 2 Market prices for electrical energy.

Time slot	Time	Electricity purchase price (yuan/MWh)	Electricity sales price (yuan/MWh)
Peak hour	8:00–12:00, 17:00–21:00	920.3	460.15
Weekday period	12:00–17:00, 21:00–24:00	622.6	311.3
Valley time	0:00–8:00	324.9	162.45

TABLE 3 Market prices for peaking ancillary services.

Peaking filling periods	Peaking filling price (yuan/MWh)	Peaking shaving periods	Peaking shaving price (yuan/MWh)
0:00–8:00	350	8:00–12:00, 17:00–21:00	500

Scenario 1: The user side participates only in the electrical energy market bidding and does not account for the uncertainty of the user-side regulation capacity.

Scenario 2: The user side participates in both the electrical energy and peaking ancillary services markets while adopting the strategy devised herein, but does not account for the user-side regulation capacity uncertainty.

Scenario 3: The user side participates only in the electrical energy market bidding, and the uncertainty of the user-side regulation capacity is considered.

Scenario 4: The user side participates in both the electrical energy and peaking ancillary services markets while adopting the strategy devised herein and taking into account the user-side regulation capacity uncertainty.

TABLE 4 User-side benefits under different scenarios.

Market gains (yuan)	Scenario 1	Scenario 2	Scenario 3	Scenario 4
Electricity market	−12,685	−9,608.7	−14,274	−10,179
FM ancillary services market	0	20,871	0	21,593
Energy storage operating costs	221.5	1,238.4	228.9	1,247.5
Aggregate return	−16,754	5,115.9	−18,287.3	5,278.7

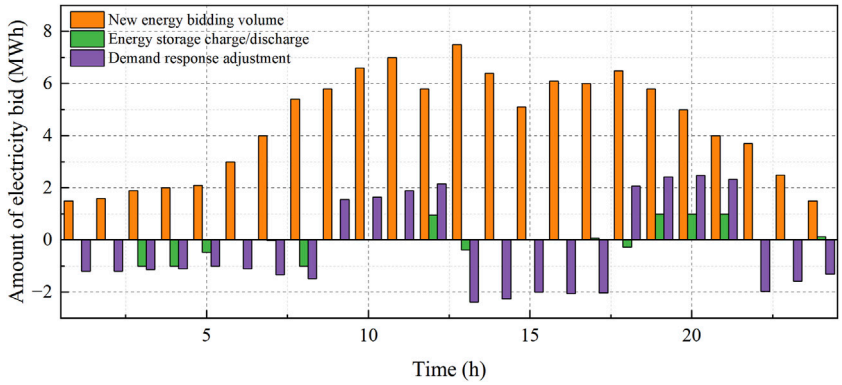

FIGURE 3
Optimization results for user-side resources under Scenario 1

Comparisons of the market returns on the customer side for different scenarios are shown in Table 4. The negative electrical energy market gains indicate that the costs of purchasing electricity on the load side are greater than the gains from selling electricity. From Table 4, it is seen that participating in the peak load balancing auxiliary service market (Scenarios 2 and 4) can significantly improve the total revenue of users compared to participating only in the electricity and energy markets (Scenarios 1 and 3). The operating costs of energy storage are relatively high in Scenarios 2 and 4, and Scenario 4 achieves the best total benefit through the strategy proposed herein when considering the uncertainty of user-side regulation capacity. It can be seen that the benefits are greatest in the scenario where the customer side participates in both the electrical energy and peak shaving auxiliary service markets. The customer side calls adjustable resources to participate in peak shaving and peak shifting to obtain peak shifting benefits while reducing the cost of purchasing electricity in the electrical energy market.

Figure 3 shows the trading strategy for the participation of user-side resources in the electrical energy market of Scenario 1, where the positive and negative values of the distributed energy storage represent the discharging and charging processes, while the positive and negative values of demand–response load adjustment represent the load curtailment and load increase, respectively. From the figure, it is seen that the user side reduces the power purchase costs through coordinated scheduling of the internal adjustable resources. Considering the high purchase prices of power in the market, the internal load supply source on the user side is mainly new energy. The energy storage is charged during the valley hours of 3:00–5:00 and discharged during the peak hours of 19:00–21:00, thus reducing the amount of power purchased during the high-price hours. As seen from the demand–response bidding bar chart, the demand–response load cuts the loads during the peak hours of 9:00–12:00 and 18:00–21:00 while increasing the loads during the valley hours of 0:00–8:00 and 22:00–24:00 to achieve peak cutting and valley filling that reduce the cost of purchasing power on the customer side.

Figure 4 shows the bidding results of Scenarios 1 and 2 for user-side participation in electrical energy trading, where a positive bidding power indicates that the user side purchases power from the electrical energy market, and a negative value indicates that the user side sells power to the market. From the figure, it is seen that the user side mainly focuses on selling electricity to the grid from 8:00 to 12:00 because the market price of electricity is higher at this time. In addition, compared with Scenario 1, the user side purchases less power in the valley time, sells more power in the peak time, and purchases more power in the normal time in Scenario 2. Figure 5 shows the optimization strategy for Scenario 2 with adjustable loads for participating in the peaking auxiliary service market. The results show that when the customer side participates in both the electrical energy and peaking auxiliary service markets, the adjustable resources will preferentially participate in the market with higher returns. For example, the participation of adjustable resources in valley filling and peaking during the valley hours of 01:00–08:00 not only increases the peaking revenue but also reduces the amount of power purchased in the electrical energy market. The energy storage discharges to participate in peak shaving and peak regulation during the peak hours of 9:00–12:00 and 18:00–21:00, while charging during the flat hours. Demand–response loads participate in valley filling and peak shaving by increasing their electricity

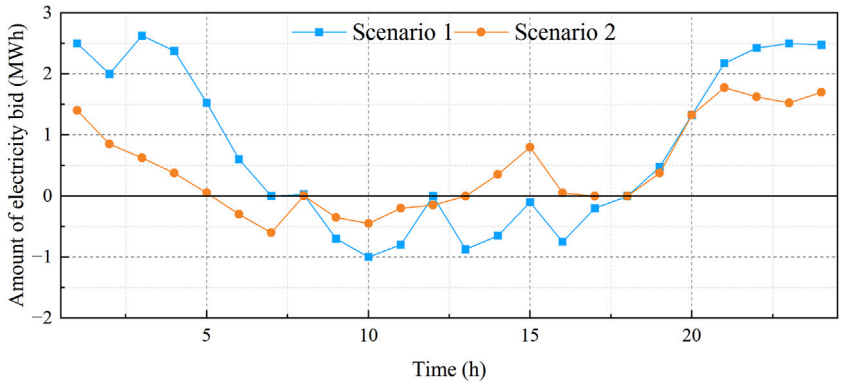

FIGURE 4
Bidding results for user-side participation in the electricity market under Scenarios 1 and 2

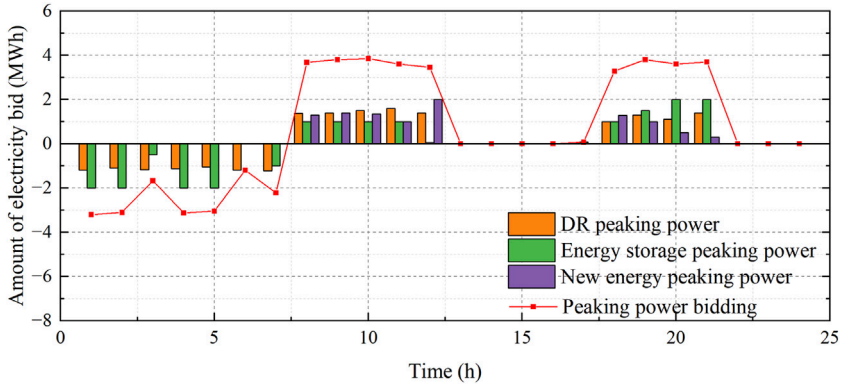

FIGURE 5
Bidding results for load-side participation in the peaking market under Scenario 2.

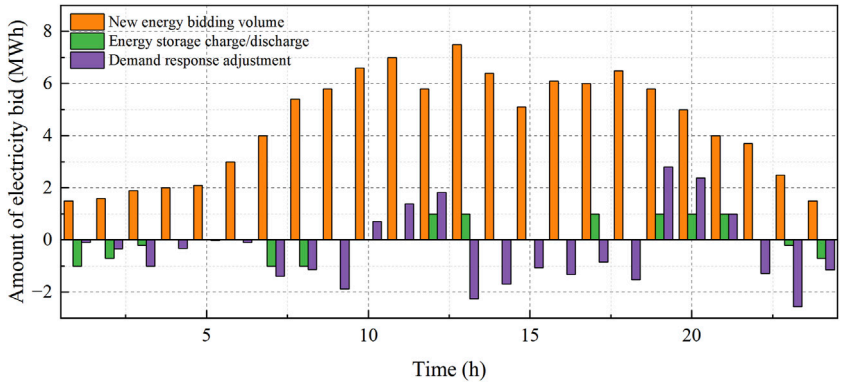

FIGURE 6
Optimization results for user-side resources under Scenario 3

consumption during the valley hours and load curtailment during the peak hours as the benefits gained from participating in peak shaving at this time are greater than the cost reductions from participating in electrical energy trading.

The optimization results for Scenarios 3 and 4 involve adjustable resources participating in the day-ahead energy market, as shown in Figures 6, 7, respectively. The bidding results for adjustable resource participation in the peaking ancillary services market for Scenario

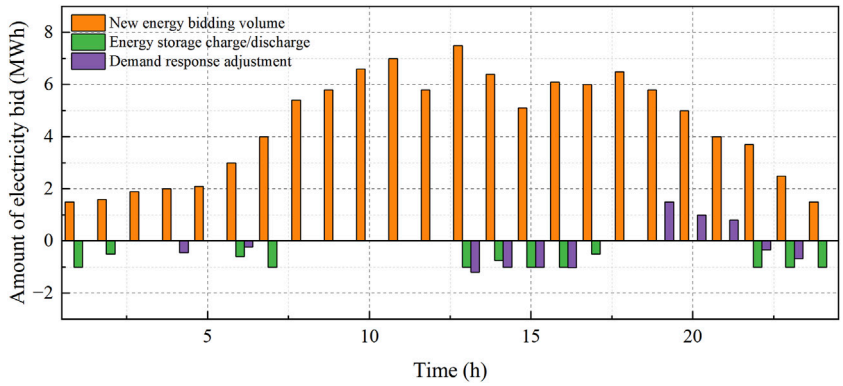

FIGURE 7
Optimization results for user-side resources under Scenario 4

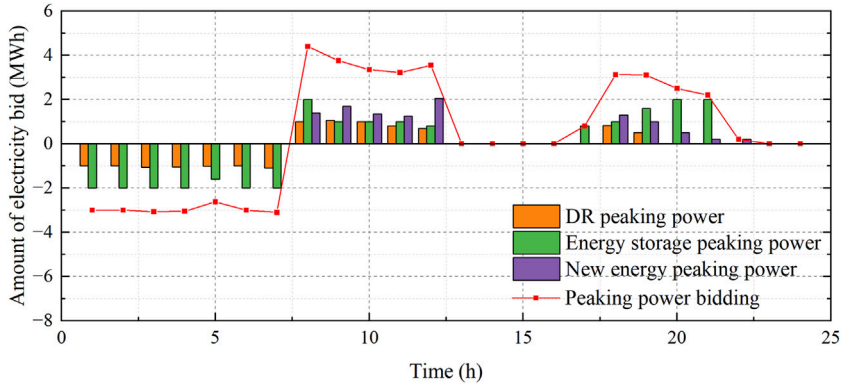

FIGURE 8
Bidding results for user-side participation in the peaking market under Scenario 4.

4 are shown in Figure 8. Compared to Scenarios 1 and 2, the demand–response load participation in the market is lower in the uncertainty scenarios, while the amount of electricity purchased in the energy market increases, thus leading to lower customer-side revenues. This is because the customer-side bidding strategy is more conservative when considering the risk of demand–response uncertainty on bidding revenues, which is preferably compensated by purchasing power in the electrical energy market or calling other flexible resources with higher controllability. In addition, the results of the comparisons between Scenarios 3 and 4 show that when more uncertainty is considered, the bidding strategy of the customer side is more conservative and capacity of the demand–response load to participate in market bidding is reduced.

5.3 Comparative analysis of uncertain optimization methods

To verify the DRCC model proposed herein under consideration of risk expectation, SO is used for comparison and analysis against RO. The SO-based decision-making method assumes that the prediction error of the demand–response load obeys a Gaussian distribution with a mean of 0 and standard deviation of 0.2; accordingly, 1,500 sets of data are sampled by the Monte Carlo method selected for analysis.

Figure 9 shows how the load-side gains vary with confidence levels and sample numbers across the models. The SO model yields the highest gains, while the RO model yields the lowest. The DRCC model's gains fall in between these and increase with more samples as the estimated distribution becomes more accurate, thus reducing decision conservatism. Moreover, the gains obtained by the user side based on the DRCC model increase with the number of samples; as more samples are included, the fuzzy centralized probability distribution tends to be closer to the true distribution, and the decision conservatism decreases. In addition, it is seen from the figure that the user-side gain decreases gradually with increase in confidence level. When the confidence level is low, the gain obtained by the DRCC model tends to be close to that of the SO model, and when the confidence level is high, the results gradually converge to those of the RO model. This is because, when the confidence level is 0, the uncertainty set includes only the empirical distribution such that the DRCC model degenerates into the SO model. As the confidence level increases, the uncertainty in the system

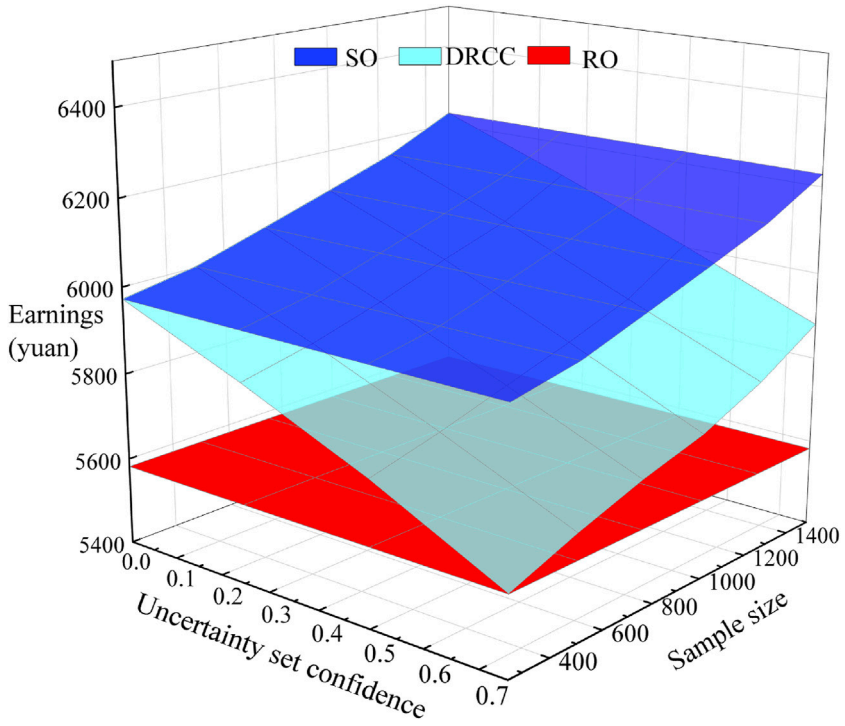

FIGURE 9
Variation of user-side returns with confidence level and sample size.

increases, which makes the model more robust and bidding strategy on the user side more conservative, thereby decreasing the corresponding gain and converging toward the RO model. The SO-based approach assumes that the demand–response prediction error obeys a given probability distribution in the fuzzy set of the DRCC model, so the conservatism is low and the user-side gains are higher. The RO-based approach considers the worst-case scenario in the demand–response uncertainty set, resulting in overly conservative RO decision results and lowest user-side gains. The DRCC model in this work does not require a specific probability distribution of the demand–response uncertainty variable and considers all possible probability distribution information to make an optimization decision based on the worst probability distribution, such that the conservatism is between those of the RO and SO approaches.

Table 5 shows the computation times of the RO, SO, and DRCC models for different numbers of samples; the results show that as the number of samples increases, the solution times of all three models increase. The computation time of the DRCC model is within 15 s and does not change drastically with a change in the number of samples, indicating that the model has good computational adaptability.

5.4 Analysis of the impact of model parameters

The confidence level β in the DRCC model indicates the level of confidence in the probability distribution of the uncertainty set, and the risk factor ε indicates the level of risk that can be tolerated by the opportunity constraints. Table 6 shows the effects of different values of the confidence level β and risk factor ε on the user-side gains. After data verification, when the confidence level increases, the user-side returns decrease; when the risk factor increases, the user-side returns increase. The results also show that the user-side gain decreases with increases in the confidence level and risk factor. This is because, as the confidence level increases and risk factor decreases, the decision-maker's risk appetite decreases, such that more controllable flexibility resources are invoked to cope with the demand–response uncertainty and the model robustness improves the gain decrease. From the above analysis, it is noted that the decision-maker can effectively balance the economy and reliability of decision-making by flexibly adjusting the confidence level and risk factor of the fuzzy uncertainty set. The policy environment of the power market, such as the pricing policies and market reforms, will also affect the selection and optimization results of the parameters in the DRCC model. For example, dynamic adjustment of the time-of-use tariff policy will directly affect the consumption behaviors and costs of the power users, thereby affecting the strategy choices of the users in the DRCC model.

6 Conclusion

In the context of the electricity market, this work proposes a joint bidding method for user-side resources to participate in both the electrical energy and peaking auxiliary service markets; we constructed a day-ahead market bidding decision model based on risk expectation and distributional robust opportunity constraints in

TABLE 5 Model solution times for different numbers of samples.

Modeling	Solution time(s) for different number of samples (s)		
	500	1,000	1,500
RO	5.05	8.53	10.02
SO	9.28	21.12	30.36
DRCC	6.78	9.39	12.51

TABLE 6 Effects of confidence level and risk factor on user-side returns.

Confidence level (math.)	Proceeds (yuan)		
	$\varepsilon = 0.05$	$\varepsilon = 0.1$	$\varepsilon = 0.15$
$\beta = 0.75$	5,730.3	5,880.4	5,936.1
$\beta = 0.95$	5,581.7	5,641.6	5,704.8

response to load uncertainties. The main conclusions of this study based on numerical validation are as follows:

1) The user-side joint bidding strategy for participation in the electrical energy and peaking auxiliary service markets based on the distributional robust opportunity constraints proposed herein can effectively cope with the bidding risk caused by user-side resource uncertainty. The user side can balance the economy and reliability of decision-making by adjusting the confidence level and risk coefficient of the fuzzy uncertainty set, which provides a high degree of flexibility. This promotes optimal allocation of power resources in the market and improves the overall energy efficiency; effective management of the user-side resource uncertainty thus helps reduce market volatility and promote long-term market stability.
2) The DRCC model constructed herein by considering risk expectation achieves better balance between robustness and economy. Compared with the RO and SO models, the DRCC model overcomes the problem of the RO model that is too conservative and has better computational adaptability than the SO model. The DRCC model reduces conservatism, avoids the problem of over-conservatism, and improves the computational adaptability. At the same time, in the power system, it enables better dispatch of the power resources, balanced supply and demand, reduction of the cost problem caused by uncertainty, enhanced adaptability of the system to different situations, and improved robustness of the entire system.
3) The present study focuses on the impacts of demand–response load uncertainties on user-side revenue; however, incorporating uncertainties regarding different types of user-side resources into the user-side bidding decision models will be the focus of subsequent research efforts. We intend to handle the uncertainty of user-side resources through SemBleu stick optimization and opportunity constraints as well as address the problems thereof using conditional risk-based approximation; we will also incorporate the uncertainties of different types of user-side resources into the user-side bidding decision model.

Data availability statement

The original contributions presented in this study are included in the article/supplementary material, and any further inquiries may be directed to the corresponding author.

Author contributions

JW: Conceptualization, Data curation, Formal Analysis, Funding acquisition, Methodology, Project administration, Resources, Software, Validation, Writing–original draft, Writing–review and editing. JH: formal Analysis, Funding Acquisition, Resources, Writing–original draft, Writing–review and editing. ZB: Investigation, Methodology, Project administration, Writing–original draft, Writing–review and editing. HH: Software, Supervision, Visualization, Writing–original draft. MT: Formal Analysis, Methodology, Writing–original draft.

Funding

The authors declare that financial support was received for the research, authorship, and/or publication of this article. This work was supported by the State Grid Inner Mongolia East Electric Power Company Economic and Technological Research Institute (Research on the benefit mechanism of source, grid, load and energy storage multi-body cooperative power transmission of energy bases in large desert, Gobi and wasteland; No. 526606230001).

Conflict of interest

The authors declare that the research was conducted in the absence of any commercial or financial relationships that could be construed as a potential conflict of interest.

The authors declare that this study received funding from State Grid Inner Mongolia East Electric Power Company Economic and Technological Research Institute. The funder had the following involvement in the study: collection, analysis, interpretation of data, the writing of this article, the decision to submit it for publication.

Publisher's note

organizations, or those of the publisher, the editors and the reviewers. Any product that may be evaluated in this article, or claim that may be made by its manufacturer, is not guaranteed or endorsed by the publisher.

References

Alabi, T. M., Lu, L., and Yang, Z. (2021). Improved hybrid inexact optimal scheduling of virtual powerplant (VPP) for zero-carbon multi-energy system (ZCMES) incorporating Electric Vehicle (EV) multi-flexible approach. *J. Clean. Prod.* 326, 129294. doi:10.1016/j.jclepro.2021.129294

Alahyari, A., Ehsan, M., and Mousavizadeh, M. (2019). A hybrid storage-wind virtual power plant (VPP) participation in the electricity markets: a self-scheduling optimization considering price, renewable generation, and electric vehicles uncertainties. *J. Energy Storage* 25, 100812. doi:10.1016/j.est.2019.100812

Al-Jabouri, H., Saif, A., Diallo, C., and Khatab, A. (2024). Distributionally-robust chance-constrained optimization of selective maintenance under uncertain repair duration. *Expert Syst. Appl.* 239, 122303. doi:10.1016/j.eswa.2023.122303

Bai, Y., Zhang, W., Yu, T., Wang, J., Deng, G., Yan, J., et al. (2023). Flexibility quantification and enhancement of flexible electric energy systems in buildings. *J. Build. Eng.* 68, 106114. doi:10.1016/j.jobe.2023.106114

Cao, Y., and Zhang, S. (2023). Facilitating the provision of load flexibility to the power system by data centers: a hybrid research method applied to China. *Util. Policy* 84, 101636. doi:10.1016/j.jup.2023.101636

Chassin, D. P., and Rondeau, D. (2016). Aggregate modeling of fast-acting demand response and control under real-time pricing. *Appl. Energy* 181, 288–298. doi:10.1016/j.apenergy.2016.08.071

Cheng, Y., Zheng, H., Juanatas, R. A., and Golkar, M. J. (2023). Profitably scheduling the energy hub of inhabitable houses considering electric vehicles, storage systems, revival provenances and demand side management through a modified particle swarm optimization. *Sustain. Cities Soc.* 92, 104487. doi:10.1016/j.scs.2023.104487

Datta, J., and Das, D. (2023). Energy management of multi-microgrids with renewables and electric vehicles considering price-elasticity based demand response: a bi-level hybrid optimization approach. *Sustain. Cities Soc.* 99, 104908. doi:10.1016/j.scs.2023.104908

Du, J., Han, X., and Wang, J. (2024). Distributed cooperation optimization of multi-microgrids under grid tariff uncertainty: a nash bargaining game approach with cheating behaviors. *Int. J. Electr. Power and Energy Syst.* 155, 109644. doi:10.1016/j.ijepes.2023.109644

Fan, W., Ju, L., Tan, Z., Li, X., Zhang, A., Li, X., et al. (2023a). Two-stage distributionally robust optimization model of integrated energy system group considering energy sharing and carbon transfer. *Appl. Energy* 331, 120426. doi:10.1016/j.apenergy.2022.120426

Fan, W., Tan, Z., Li, F., Zhang, A., Ju, L., Wang, Y., et al. (2023b). A two-stage optimal scheduling model of integrated energy system based on CVaR theory implementing integrated demand response. *Energy* 263, 125783. doi:10.1016/j.energy.2022.125783

Guo, H., Davidson, M. R., Chen, Q., Zhang, D., Jiang, N., Xia, Q., et al. (2020). Power market reform in China: motivations, progress, and recommendations. *Energy Policy* 145, 111717. doi:10.1016/j.enpol.2020.111717

Hasan, M., Mifta, Z., Salsabil, N. A., Papiya, S. J., Hossain, M., Roy, P., et al. (2023). A critical review on control mechanisms, supporting measures, and monitoring systems of microgrids considering large scale integration of renewable energy sources. *Energy Rep.* 10, 4582–4603. doi:10.1016/j.egyr.2023.11.025

Jin, Y., Amoasi Acquah, M., Seo, M., Ghorbanpour, S., Han, S., and Jyung, T. (2023). Optimal EV scheduling and voltage security via an online bi-layer steady-state assessment method considering uncertainties. *Appl. Energy* 347, 121356. doi:10.1016/j.apenergy.2023.121356

Khodadadi, A., Söder, L., and Amelin, M. (2022). Stochastic adaptive robust approach for day-ahead energy market bidding strategies in hydro dominated sequential electricity markets. *Sustain. Energy, Grids Netw.* 32, 100827. doi:10.1016/j.segan.2022.100827

Khorasany, M., Shokri Gazafroudi, A., Razzaghi, R., Morstyn, T., and Shafie-khah, M. (2022). A framework for participation of prosumers in peer-to-peer energy trading and flexibility markets. *Appl. Energy* 314, 118907. doi:10.1016/j.apenergy.2022.118907

Li, C., Wang, X., Li, J., Zhu, X., Yan, G., and Jia, C. (2023a). Multi-constrained optimal control of energy storage combined thermal power participating in frequency regulation based on life model of energy storage. *J. Energy Storage* 73, 109050. doi:10.1016/j.est.2023.109050

Li, Y., Deng, Y., Wang, Y., Jiang, L., and Shahidehpour, M. (2023b). Robust bidding strategy for multi-energy virtual power plant in peak-regulation ancillary service market considering uncertainties. *Int. J. Electr. Power and Energy Syst.* 151, 109101. doi:10.1016/j.ijepes.2023.109101

Li, Y., Zhang, J., Wu, X., Shen, J., and Maréchal, F. (2023c). Stochastic-robust planning optimization method based on tracking-economy extreme scenario tradeoff for CCHP multi-energy system. *Energy* 283, 129025. doi:10.1016/j.energy.2023.129025

Liang, Y., Lin, S., Feng, X., Liu, M., Su, L., and Zhang, B. (2023). Optimal resilience enhancement dispatch of a power system with multiple offshore wind farms considering uncertain typhoon parameters. *Int. J. Electr. Power and Energy Syst.* 153, 109337. doi:10.1016/j.ijepes.2023.109337

Lin, Q., Lu, S., Yue, L., and Guo, T. (2023). A two-stage optimization method for improving the load flexibility of existing district energy systems. *Energy Build.* 301, 113680. doi:10.1016/j.enbuild.2023.113680

Mei, S., Tan, Q., Liu, Y., Trivedi, A., and Srinivasan, D. (2023). Optimal bidding strategy for virtual power plant participating in combined electricity and ancillary services market considering dynamic demand response price and integrated consumption satisfaction. *Energy* 284, 128592. doi:10.1016/j.energy.2023.128592

Ordoudis, C., Nguyen, V. A., Kuhn, D., and Pinson, P. (2021). Energy and reserve dispatch with distributionally robust joint chance constraints. *Operations Res. Lett.* 49, 291–299. doi:10.1016/j.orl.2021.01.012

Pan, L., Xu, X., Yang, Y., Liu, J., and Hu, W. (2023). Distributionally robust economic scheduling of a hybrid hydro/solar/pumped-storage system considering the bilateral contract flexible decomposition and day-ahead market bidding. *J. Clean. Prod.* 428, 139344. doi:10.1016/j.jclepro.2023.139344

Qin, Y., Rao, Y., Xu, Z., Lin, X., Cui, K., Du, J., et al. (2023). Toward flexibility of user side in China: virtual power plant (VPP) and vehicle-to-grid (V2G) interaction. *eTransportation* 18, 100291. doi:10.1016/j.etran.2023.100291

Roald, L. A., Pozo, D., Papavasiliou, A., Molzahn, D. K., Kazempour, J., and Conejo, A. (2023). Power systems optimization under uncertainty: a review of methods and applications. *Electr. Power Syst. Res.* 214, 108725. doi:10.1016/j.epsr.2022.108725

Sarfarazi, S., Mohammadi, S., Khastieva, D., Hesamzadeh, M. R., Bertsch, V., and Bunn, D. (2023). An optimal real-time pricing strategy for aggregating distributed generation and battery storage systems in energy communities: a stochastic bilevel optimization approach. *Int. J. Electr. Power and Energy Syst.* 147, 108770. doi:10.1016/j.ijepes.2022.108770

Schwidtal, J. M., Agostini, M., Coppo, M., Bignucolo, F., and Lorenzoni, A. (2023). Optimized operation of distributed energy resources: the opportunities of value stacking for Power-to-Gas aggregated with PV. *Appl. Energy* 334, 120646. doi:10.1016/j.apenergy.2023.120646

Tan, Z., Wang, G., Ju, L., Tan, Q., and Yang, W. (2017). Application of CVaR risk aversion approach in the dynamical scheduling optimization model for virtual power plant connected with wind-photovoltaic-energy storage system with uncertainties and demand response. *Energy* 124, 198–213. doi:10.1016/j.energy.2017.02.063

Xie, Y., Wu, X., Hou, Z., Li, Z., Luo, J., Lüddeke, C. T., et al. (2023). Gleaning insights from German energy transition and large-scale underground energy storage for China's carbon neutrality. *Int. J. Min. Sci. Technol.* 33, 529–553. doi:10.1016/j.ijmst.2023.04.001

Zhang, G., Jia, N., Zhu, N., He, L., and Adulyasak, Y. (2023). Humanitarian transportation network design via two-stage distributionally robust optimization. *Transp. Res. Part B Methodol.* 176, 102805. doi:10.1016/j.trb.2023.102805

Zhang, J., and Liu, Z. (2023). Low carbon economic dispatching model for a virtual power plant connected to carbon capture system considering green certificates-carbon trading mechanism. *Sustain. Energy Technol. Assessments* 60, 103575. doi:10.1016/j.seta.2023.103575

Zhang, W., Yan, C., Xu, Y., Fang, J., and Pan, Y. (2022). A critical review of the performance evaluation and optimization of grid interactions between zero-energy buildings and power grids. *Sustain. Cities Soc.* 86, 104123. doi:10.1016/j.scs.2022.104123